Biochemical and Biophysical Research Communications 456 (2015) 835–840

Contents lists available at ScienceDirect

Biochemical and Biophysical Research Communications

journal homepage: www.elsevier.com/locate/ybbrc

Blockage of mitochondrial calcium uniporter prevents iron accumulation in a model of experimental subarachnoid hemorrhage

Huiying Yan [a], Shuangying Hao [b], Xiaoyan Sun [b], Dingding Zhang [a], Xin Gao [a], Zhuang Yu [a], Kuanyu Li [b,*], Chun-Hua Hang [a,*]

[a] Department of Neurosurgery, Jinling Hospital, School of Medicine, Nanjing University, 305 East Zhongshan Road, Nanjing 210002, Jiangsu Province, China
[b] Jiangsu Key Laboratory for Molecular Medicine, Medical School of Nanjing University, 22 Hankou Road, Nanjing 210093, Jiangsu Province, China

ARTICLE INFO

Article history:
Received 11 December 2014
Available online 19 December 2014

Keywords:
Subarachnoid hemorrhage
Mitochondrial calcium uniporter
Iron accumulation
Brain injury

ABSTRACT

Previous studies have shown that iron accumulation is involved in the pathogenesis of brain injury following subarachnoid hemorrhage (SAH) and chelation of iron reduced mortality and oxidative DNA damage. We previously reported that blockage of mitochondrial calcium uniporter (MCU) provided benefit in the early brain injury after experimental SAH. This study was undertaken to identify whether blockage of MCU could ameliorate iron accumulation-associated brain injury following SAH. Therefore, we used two reagents ruthenium red (RR) and spermine (Sper) to inhibit MCU. Sprague–Dawley (SD) rats were randomly divided into four groups including sham, SAH, SAH + RR, and SAH + Sper. Biochemical analysis and histological assays were performed. The results confirmed the iron accumulation in temporal lobe after SAH. Interestingly, blockage of MCU dramatically reduced the iron accumulation in this area. The mechanism was revealed that inhibition of MCU reversed the down-regulation of iron regulatory protein (IRP) 1/2 and increase of ferritin. Iron–sulfur cluster dependent-aconitase activity was partially conserved when MCU was blocked. In consistence with this and previous report, ROS levels were notably reduced and ATP supply was rescued; levels of cleaved caspase-3 dropped; and integrity of neurons in temporal lobe was protected. Taken together, our results indicated that blockage of MCU could alleviate iron accumulation and the associated injury following SAH. These findings suggest that the alteration of calcium and iron homeostasis be coupled and MCU be considered to be a therapeutic target for patients suffering from SAH.

1. Introduction

Aneurysmal subarachnoid hemorrhage (SAH) makes up only 5% of all strokes but has high morbidity and mortality rates [1]. The majority of deaths occur within the first few days, thus early brain injury (EBI) has been supposed to be the most important factor determining the prognosis of patients suffering from SAH [2]. Various mechanisms are involved in the pathogenesis of EBI after SAH, including oxidative stress, apoptosis, and impaired iron homeostasis [3].

Blood released into the subarachnoid space clots almost immediately and the amount of blood correlates with neurologic deficits and poor clinical outcome [4]. Hemoglobin (Hgb) and its oxidation product, heme, are released. Heme is converted in brain by heme oxygenase (HO) into carbonmonoxide, biliverdin and iron [5]. Recent studies indicate that oxidative injury caused by excessive hemoglobin and iron overload contributes significantly to brain damage after intracerebral hemorrhage (ICH) [6]. Besides, overloaded iron plays an important role in neurodegenerative diseases, for example Alzheimer's disease and Parkinson's diseases [7,8]. An excess of iron can be toxic because it has the ability to accept and donate electrons by exchanging between ferrous and ferric forms. This exchanging may generate reactive oxygen species (ROS) through Fenton reactions, causing oxidative stress and organic biomolecule oxidation [9]. The previous study has demonstrated that large amounts of iron arising from hemoglobin degradation might

Abbreviations: DMT1, divalent metal transporter 1; EBI, early brain injury; Ft, ferritin; Fpn-1, ferroportin-1; IRP, iron regulatory protein; IREs, iron-responsive elements; IRE-BPs, iron-responsive element-binding proteins; ISCU, iron–sulfur cluster scaffold protein; MCU, mitochondrial calcium uniporter; PBS, phosphate buffer solution; ROS, reactive oxygen species; RR, ruthenium red; Sper, spermine; SD, Sprague–Dawley; SAH, subarachnoid hemorrhage; Tf, transferrin; TfR, transferrin receptor.

* Corresponding authors. Fax: +86 25 80863310 (C.-H. Hang).
E-mail addresses: likuanyu@nju.edu.cn (K. Li), hang_neurosurgery@163.com (C.-H. Hang).

http://dx.doi.org/10.1016/j.bbrc.2014.12.073
0006-291X/

participate in the generation of free radicals leading to increased oxidative injury and DNA damage after SAH. Systemic administration of deferoxamine, an iron chelator, could reduce iron level and iron-handling proteins, and significantly ameliorated oxidative injury and neuronal cell death [10].

Mitochondrial calcium uniporter (MCU) locates in the inner membrane of mitochondria. It can be inhibited by ruthenium red (RR) and opened by polyamine like spermine (Sper) [11,12]. However, in our previous study, not only RR but also Sper worked as an inhibitor of MCU [13]. Under normal conditions, Ca^{2+} enters mitochondria through MCU. Past studies have demonstrated that blockage of MCU could prevent mitochondrial dysfunction caused by iron overload both in brain and heart [14,15]. In our previous study, we have demonstrated that blockage of MCU could prevent intracellular calcium accumulation, thus alleviate early brain injury following SAH [13]. The purpose of this study is to verify whether blockage of MCU could prevent iron accumulation following SAH.

2. Materials and methods

2.1. Animal preparation

All procedures were approved by the Animal Care and Use Committee of Nanjing University and were conformed to guide for the Care and Use of Laboratory Animals by National Institutes of Health. Male Sprague–Dawley (SD) rats (6–8 weeks, 270–330 g) were obtained from Animal Center of Jinling hospital (Nanjing, China). The rats were housed in a humidity controlled room (25 ± 1 °C, 12 h light/dark cycle) and were raised with free access to water and food.

2.2. Experimental design

Total 60 rats were randomly divided into the sham (surgery with normal saline insult, $n = 15$), SAH ($n = 15$), SAH + RR (SAH treated with RR 2.5 mg/kg, $n = 15$) and SAH + Sper (SAH treated with Sper 5 mg/kg, $n = 15$) groups. RR or Sper (both from Sigma, USA, dissolved in sterile saline solution) were injected directly intraperitoneally (IP) at 15 min after SAH. Notably, the dose of 2.5 mg/kg RR and 5 mg/kg Sper was previously determined to be the optimal dosage for producing neuroprotective effects in our previous study in rats [13]. None treatments were administered in the sham and SAH groups. Six rats from each group were selected randomly to take temporal cortex for the analysis of ATP, ROS, western blot, aconitase activity and histological assays at Day 1 after SAH.

2.3. Prechiasmatic cistern blood injection for SAH model

Experimental SAH models were performed as reported previously [16–18]. The rats were anesthetized with chloral hydrate (0.4 mg/kg, IP, Jinling hospital). The hair on the head and near the inguinal region was carefully shaved and then the rats were positioned prone in a stereotactic frame. After disinfection, a midline scalp incision was made and a 1 mm hole was drilled 8.0 mm anterior to the bregma in the midline of the skull, through the skull bone, down to duramater without perforating the underlying matter. Then the animals were positioned supination. After disinfection again we use insulin injection needle (BD Science, Franklin Lakes, NJ) to draw 300 μl volume of blood from femoral artery. The needle was advanced 11 mm into the prechiasmatic cistern through the burr hole, at a 45° angle to the vertical plane, and the 300 μl blood was injected into the prechiasmatic cistern over 20 s. Loss of cerebrospinal fluid and bleeding from the midline vessels were prevented by plugging the burr hole with bone wax prior to inserting the needle. Sham animals were injected with 300 μl normal saline. After injection, animals were kept in a 30 °C, heads-down position for 20 min. After recovery from anesthesia, the rats were returned to their cages and housed at 25 ± 1 °C. Rats that died during surgery or during surgical recovery were excluded, and the procedure was repeated until final group sizes reached the planned experimental number.

2.4. Perfusion–fixation and tissue preparation

Animals were anesthetized as above, and perfused through the left cardiac ventricle with normal saline (4 °C) until effluent from the right atrium was clear. Animals, which had obvious clots in the prechiasmatic cisterns, were selected to be further analyzed. The temporal lobe tissue, which was near the hematoma, was harvested on ice after blood clots on the tissue cleared carefully. The fresh tissues were used for measurement of cellular stored in -80 °C till further use for western blot and aconitase activity assays. For histological examination, the rats were perfused with normal saline (4 °C) followed by 4% buffered paraformaldehyde (4 °C) and then the brains were immersed in 4% buffered paraformaldehyde (4 °C) for further study.

2.5. Iron staining

Seven-micrometer frozen sections were used to detect the ferric iron in brain. The sections were washed with phosphate buffer solution (PBS) and then incubated in the dark with fresh-made Prussian blue staining solution (2% $K_4[Fe(CN)_6]$ and 2% HCl) for 1 h. After being washed with PBS again, the sections were incubated in the dark with fresh-made diaminobenzidine solution (30 mg DAB tablet, 40 mL 1 M Tris pH7.5, 1 mL 3% H_2O_2). At last, the sections were mounted in glycerinum. Pictures were taken under the light microscope (at 400× magnification) by an investigator blinded to the grouping. Five pictures from each section were taken and quantitation was performed using ImageJ software.

2.6. Western blot analysis

Western blot analysis was conducted as previously described [19]. Briefly, cerebral tissues were completely homogenized using lysis buffer (Thermo Fisher scientific Inc., Waltham, MA) followed by centrifugation at 14, 000×g for 15 min at 4 °C. The supernatant was collected as the total protein extraction. Protein concentration was determined with a BCA kit (Beyotime, Haimen, China) and proteins were normalized to 60 μg per lane for ferritin (Ft), transferrin receptor (TfR), ferroportin-1 (Fpn-1), iron regulatory protein (IRP) 1/2 and iron–sulfur cluster scaffold protein (ISCU) analysis. The samples were subjected to electrophoresis on 12% SDS–polyacrylamide gels for 30 min at 80 V followed by 100 min at 100 V and then transferred onto nitrocellulose membrane (NC, PALL, Port Washington, NY) sheets for 90 min at 250 mA. After blocked with 5% skim milk for 90 min at room temperature, the sheets were incubated at 4 °C overnight with primary antibodies against Ft (1:1000 dilution, Santa Cruz Biotechnology, Santa Cruz, CA), TfR (1:1000), Fpn 1 (1:1000), IRP1 (1:1000), IRP2 (1:1000), ISCU (1:1000), cleaved caspase-3 (1:500, Cell Signaling Technology, Beverly, MA), or β-tubulin (1:2,000, Sigma–Aldrich, St. Louis, MO). Antibodies used in this study were purchased from Abcam (Abcam, Cambridge, MA) if not specified. Then, the membranes were washed with tween 20 in Tris-buffered saline (TTBS, 100 mM Tris–HCl, pH 7.5, 0.9% NaCl, 0.1% Tween 20). After incubation with secondary antibodies and washing again, the blotted protein bands were visualized by enhanced chemiluminescence western blot detection reagents (Thermo Fisher scientific Inc.). Relative changes

in protein expression were estimated from the mean pixel density using ImageJ software, normalized to β-tubulin, and calculated as target protein expression/β-tubulin ratios.

2.7. Aconitase activity assays

Aconitase activity assays were performed as described previously [20,21]. Briefly, aconitase activity gels are composed of a separating gel containing 8% acrylamide, 132 mM Tris base, 132 mM borate, 3.6 mM citrate, and a stacking gel containing 4% acrylamide, 67 mM Tris base, 67 mM borate, 3.6 mM citrate. The running buffer contains 25 mM Tris (pH 8.3), 192 mM glycine, and 3.6 mM citrate. Electrophoresis was carried out at 180 V at 4 °C. Aconitase activities were visualized by incubating the gel in the dark at 37 °C in 100 mM Tris (pH 8.0), 1 mM NADP, 2.5 mM cis-aconiticacid, 5 mM MgCl2, 1.2 mM MTT, 0.3 mM phenazinemetho sulfate, and 5 U/ml isocitrate dehydrogenase. Quantitation was performed using ImageJ software.

2.8. Measurement of cellular ATP and ROS levels

Cellular ATP levels were measured using a firefly luciferase-based ATP assay kit (Beyotime) and cellular ROS levels were analyzed based on a fluorescence technique (Genmed Scientifics Inc., USA) according to the given protocols.

2.9. Nissl staining and cell counting

For Nissl staining, the 4 μm sections were hydrated in 1% toluidine blue at 50 °C for 20 min. After rinsing with double distilled water, the sections were dehydrated and mounted with permount. Normal neurons have relatively big cell body, rich in cytoplasm, with one or two big round nuclei, while damaged cells show shrunken cell bodies, condensed nuclei, dark cytoplasm, and many empty vesicles.

2.10. Statistical analysis

All data were presented as mean ± SD. SPSS 17.0 was used for statistical analysis of the data. All data were subjected to one-way ANOVA. Differences between experimental groups were determined by the Fisher's LSD post-test. Statistical significance was inferred at $p < 0.05$.

3. Results

3.1. SAH induced cellular iron accumulation and RR and Sper administration partially reversed the effect

Cellular iron homeostasis is essential for physiological cell function and tightly regulated by transferrin–transferrin receptor (Tf–TfR) internalization for iron uptake, transporter Fpn1 for iron export, and ferritin for iron storage. In the present study, iron staining proved that cellular iron was accumulated after SAH (Fig. 1A). Besides, TfR protein levels were observed to obviously increase and the levels of Fpn-1 were down-regulated (Fig. 1B), indicating that more iron was transported into the brain cells, while less iron was released. Consistent with the previous study [10], protein levels of Ft increased markedly at Day 1 after SAH in our study (Fig. 1B). Treatment with RR or Sper could significantly alleviate iron accumulation and decreased the expression of Ft, however could not influence the expression of TfR and Fpn-1 compared with the SAH group (Fig. 1B), indicating that cellular iron accumulation caused by SAH was partially reversed by blockage of MCU.

3.2. SAH-induced disruption of cellular iron homeostasis was improved by RR and Sper

Iron regulatory proteins (IRP1 and IRP2) are iron sensors to regulate the expression of iron-related proteins, for instance TfR, Fpn1, and Ft in this study, by binding to iron-responsive elements (IRE) of their mRNAs. To further verify the iron status of temporal lobe tissue, western blot analysis was performed (Fig. 2). The results showed that the levels of IRP1/2 decreased after SAH, confirming the iron accumulation in the brain. Treatment with RR and Sper could obviously restore IRP1/2 levels compared to the SAH group. These results suggested that SAH-induced disruption of cellular iron homeostasis could be reversed by blockage of MCU.

3.3. SAH-induced oxidative damage and energy supply-deficiency were recovered after SAH by RR and Sper

Abnormal iron homoeostasis can induce cellular damage through hydroxyl radical production and influence the energy supply of the cells [22]. Therefore, we measured the levels of ROS and ATP production. The results showed that ROS generation increased significantly after SAH, and this increase was markedly reduced by systemic treatment with RR and Sper (Fig. 3C). In consistence with that, energy crisis occurred following SAH and it was significantly alleviated by administration of RR and Sper (Fig. 3D).

Iron–sulfur cluster (Fe–S) directly participates in cell energy metabolism via iron–sulfur proteins in complex I/II/III. Here we measured the protein level of ISCU, a major scaffold protein for Fe–S biogenesis, and activities of aconitase, a Fe–S enzyme catalyzing the stereo-specific isomerization of citrate to isocitrate via cis-aconitate in the tricarboxylic acid cycle (Fig. 3A and B). After SAH, ISCU levels decreased and aconitase activity was notably decreased. Treatment with RR and Sper could obviously prevent the decrease of ISCU and protect aconitase activity.

3.4. Blockage of MCU by RR and Sper alleviated apoptosis and brain injury following SAH

Most animal studies have demonstrated that apoptosis is one of the most important modes of cell death post SAH. Western blot was used to detect the expression of cleaved caspase-3. Cleaved caspase-3 production increased obviously after SAH compared with the sham group and this increase was remarkably attenuated to a great extent by systemic administration with RR or Sper (Fig. 4A). In addition, Nissl staining was applied to illustrate the number and morphology change of the remained neurons in the cortex (Fig. 4B). In the sham group, rare injured neurons were detected. The visual field was full of clear and intact neurons, without edema around the cells. While a significantly great proportion of neurons in the SAH group were damaged, exhibiting extensive degenerative changes including sparse cell arrangements, loss of integrity, shrunken cytoplasma, oval or triangular nucleus, and swollen cell bodies. In contrast, the severity of neuronal degeneration in the SAH + RR and SAH + Sper groups was evidently alleviated compared to that in the SAH group.

4. Discussion

The present study provides evidence for that intraperitoneal administration of RR and Sper could alleviate iron accumulation and reverse the associated injury following SAH to a great extent.

Iron is essential for all eukaryotes, where it is used in the synthesis of heme, iron–sulfur, and other cofactors. Fe–S proteins are involved in catalysis, redox reactions, respiration, DNA replication, and transcription [23]. However, excess iron in the cells is toxic

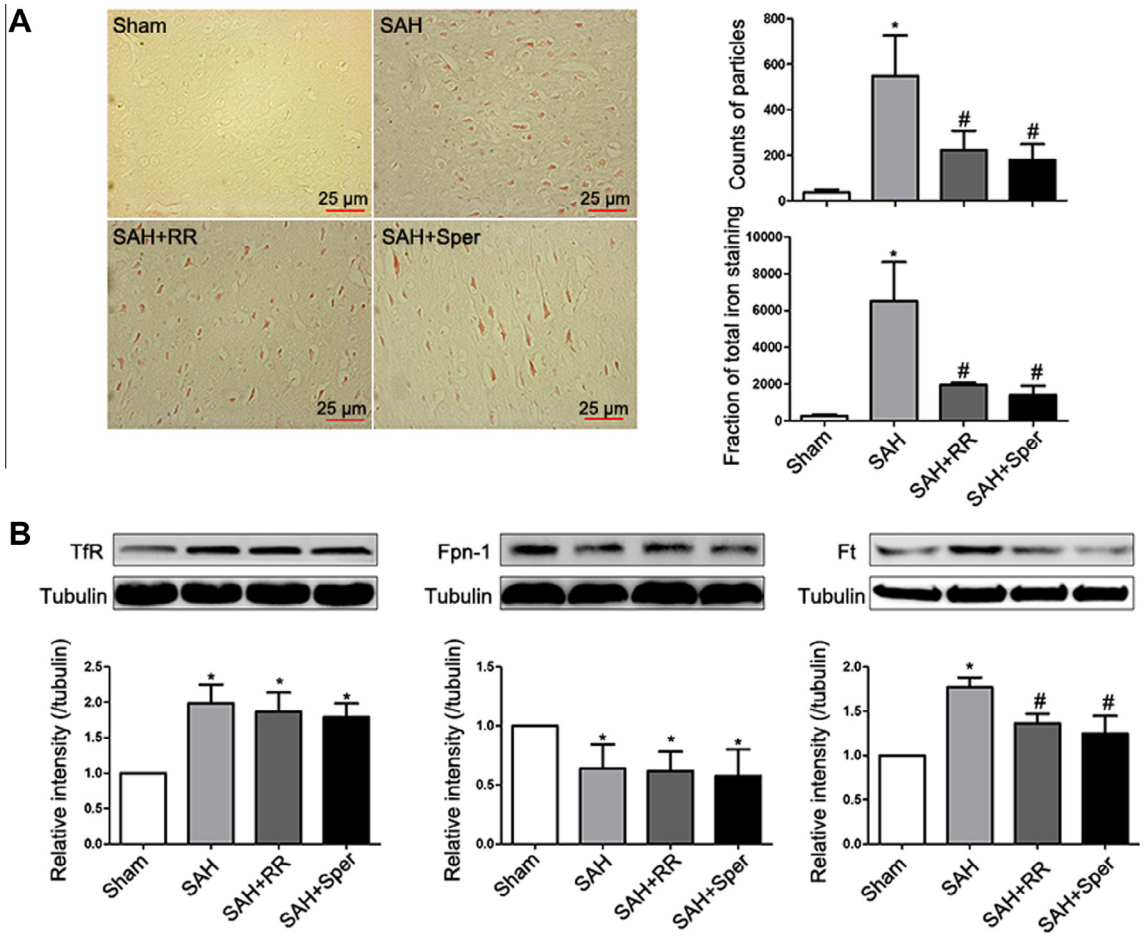

Fig. 1. SAH induced cellular iron accumulation and RR and Sper administration partially reversed the effects. (A) Iron staining of the temporal cortex. 300 μl arterial blood (normal saline in the sham group) was injected into the prechiasmatic cistern in the SAH rats. RR (2.5 mg/kg) and Sper (5 mg/kg) were given intraperitoneally at 15 min after SAH in the SAH + RR and SAH + Sper groups. The temporal cortex was harvested 1 day after SAH. The left panel shows representative brain sections of the temporal cortex with iron stained (brown) cells. The right panel is quantification of the digitized images showing the count of particles and fraction of total iron staining in each group. (B) Western blot of TfR, Fpn-1 and Ft of the brain. The upper panel shows representative protein levels of TfR, Fpn-1 and Ft. Tubulin was detected as a loading control. The bottom panel shows quantitative data of proteins TfR, Fpn-1, and Ft, respectively. Data are expressed as mean ± SD ($n = 4$ in each group). The scale bar = 25 mm. $^{*}p < 0.05$ compared with the sham group, $^{\#}p < 0.05$ compared with the SAH group. SAH, subarachnoid hemorrhage; Ft, ferritin; Fpn-1, ferroportin-1; TfR, transferrin receptor; Sper, spermine; RR, ruthenium red. (For interpretation of the references to color in this figure legend, the reader is referred to the web version of this article.)

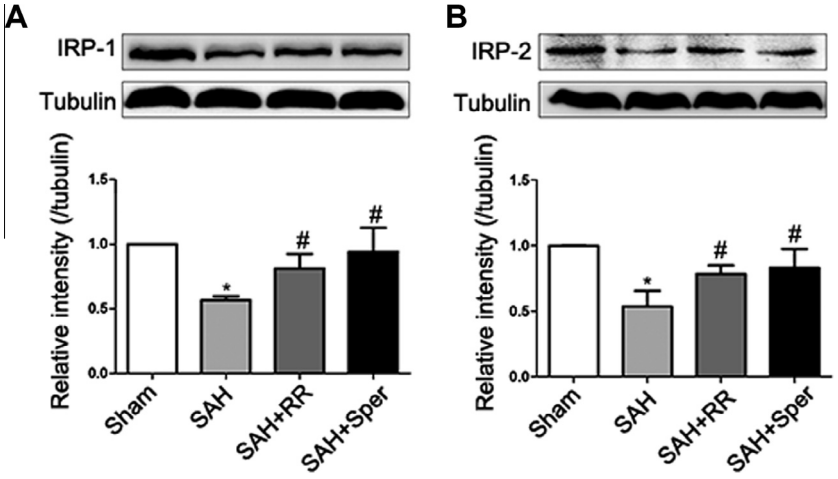

Fig. 2. SAH-induced disruption of cellular iron homeostasis was improved by RR and Sper. Western blots show IRP1 (A) and IRP2 (B) levels following SAH. The upper panel shows representative protein levels of IRP1 and IRP2. The bottom panels are quantitative data. Tubulin was used as a loading control. Data are expressed as mean ± SD ($n = 4$ in each group). $^{*}p < 0.05$ compared with the sham group, $^{\#}p < 0.05$ compared with the SAH group. IRP, iron regulatory protein. Definition of SAH, SAH + RR, and SAH + Sper groups is the same as in Fig. 1.

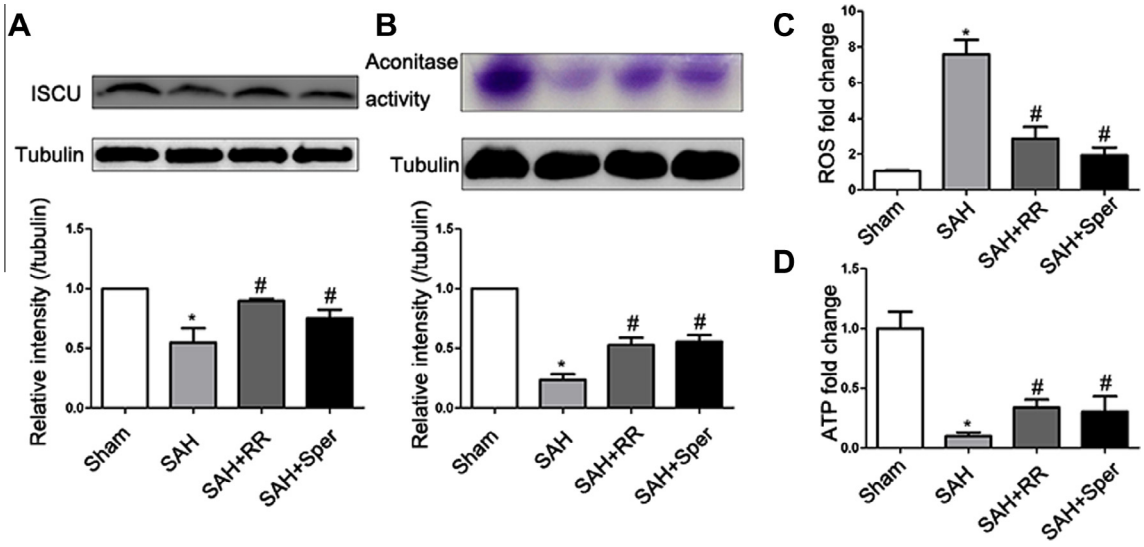

Fig. 3. SAH-induced oxidative damage and mitochondrial function were recovered by RR and Sper after SAH. Western blot and an ingel assay show protein of ISCU (A) and aconitase activity (B). The upper panels show representative results. The bottom panels show the quantitative data. ROS production (C) ATP levels (D) were measured. Data are expressed as mean ± SD ($n = 4$ in each group). $^{*}p < 0.05$ compared with the sham group, $^{\#}p < 0.05$ compared with the SAH group. ISCU, iron–sulfur cluster scaffold protein; ATP, adenosine triphosphate; ROS, reactive oxygen species. Definition of SAH, SAH + RR, and SAH + Sper groups is the same as in Fig. 1.

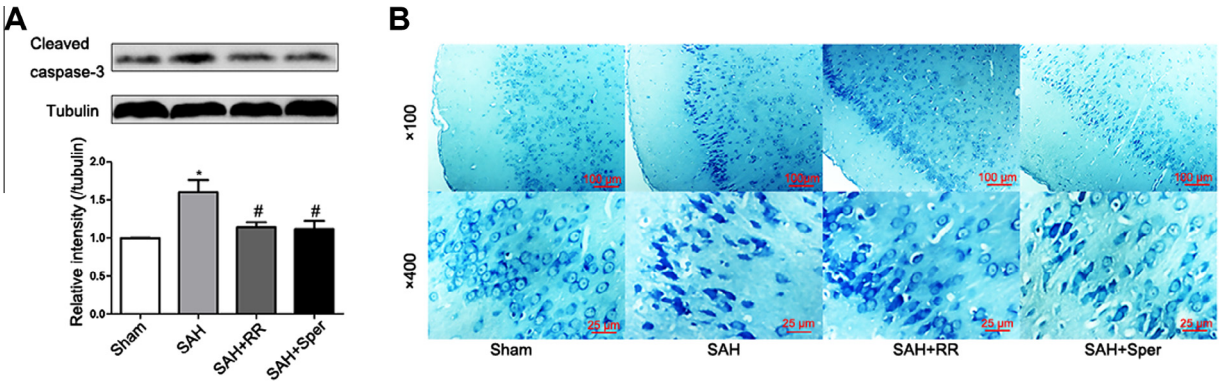

Fig. 4. Blockage of MCU by RR and Sper alleviated apoptosis and brain injury following SAH. (A) Western blot shows the levels of cleaved caspase-3 following SAH. The upper panel shows representative result. The bottom panel shows quantitative data. (B) Representative slides of Nissl staining at two different magnifications (the upper panel, 100×; the bottom panel, 400×) to visualize the neuronal cell outline and structure. SAH reduced the number of the neurons, and treatment of RR or Sper preserved neurons from damage, including neuron loss and degeneration: cells were arranged sparsely, and the cell outline was fuzzy, compared to sham group. Data are expressed as mean ± SD ($n = 5$ in each group). The scale bar in the upper panel = 100 μm and in the under panel = 25 μm. $^{*}p < 0.05$ compared with the sham group, $^{\#}p < 0.05$ compared with the SAH group. Definition of SAH, SAH + RR, and SAH + Sper groups is the same as in Fig. 1.

and iron accumulation in the adult brain is known to cause neurodegeneration [24,25]. Owing to iron's ability to donate electrons to oxygen, increased iron levels can lead to the formation of hydroxyl radicals and hydroxyl anions via the Fenton Reaction ($Fe^{2+} + H_2O_2 \rightarrow Fe^{3+} + OH + OH^-$). Thus, prevention of cellular iron from influx could alleviate ROS associated injury. The previous studies have indicated that MCU might facilitate mitochondrial Fe^{2+} influx [14,15]. Consistently in this study, blockage of MCU remarkably alleviated iron overload. As a result, ROS production decreased and cellular energy supply was improved. Consequently, RR and Sper protected the neurons from injury, which is very important for a long-term neurological improvement suffering from SAH.

Iron homeostasis is tightly regulated to avoid iron toxicity or iron deficiency. Key proteins involved in iron metabolism are regulated post-transcriptionally by the IRE–IRP system in mammalian cells. IRPs are cytosolic iron-sensing proteins that, when cells are depleted on iron, interact with RNA transcripts containing a stem loop structure known as an IRE. IREs are present in many key proteins involved in iron acquisition, transport, and storage. Low cytosolic iron levels cause two homologous IRPs (IRP1 and IRP2) to inhibit Ft and Fpn-1 translation and to stabilize mRNA transcripts of TfR and divalent metal transporter 1 (DMT1) [26]. In iron replete cells, neither IRP1 nor IRP2 binds IREs and Ft/Fpn-1 expression increases while TfR/DMT1 expression decreases [27]. After SAH, a large amount of iron arising from hemoglobin degradation was released into the subarachnoid space and more iron was transported into the cells. Thus, IRPs would be not stable and degradated. Here, IRP1 degradation could be more due to the increased ROS production induced by SAH, while IRP2 due to the accumulated cellular iron. Therefore, the protein levels of IRPs decreased, as anticipated, Ft increased obviously. Unexpectedly the protein levels of TfR and Fpn-1 did not drop after MCU blocked. This might due to the fact that too much iron was quickly released into the subarachnoid space and iron influx dominated during the acute phase following SAH. Blockage of MCU could partially protect mitochondria and give a signal by an unknown mechanism to cells to take up less iron, which reduced ROS generation. In consistence with that, IRPs and Ft levels were obviously restored by adminis-

tration of RR and Sper. Nonetheless, RR and Sper treatment did not influence the expression of TfR and Fpn-1 compared to the SAH group.

MCU locates in the inner membrane of mitochondria and facilitates Ca^{2+} uptake into mitochondria [12]. Other ions may also use MCU as a portal for uptake in mitochondria [14,15]. Blockage of MCU might prevent mitochondrial Fe^{2+} influx to protect mitochondria from iron accumulation and regulate iron homeostasis at the subcellular level. As a result, iron–sulfur cluster biogenesis was restored to regulate and sense the iron signaling by blockage of MCU after SAH [28]. Consequently, cellular iron uptake was diminished, which contributed, at least partially if not all, to protection of neurons from damage.

Collectively, this study suggested that iron accumulation was involved in the acute phase following SAH. Blockage of MCU could attenuate cellular iron accumulation, thus decrease ROS generation and improve cell energy supply, as a result, to alleviate apoptosis and brain injury following SAH. Consistent with our previous study, MCU may be a potential therapeutic target for patients suffering from SAH.

Acknowledgment

This study was supported by the National Natural Science Foundation, China (Nos. 81371294, 31071085, 31371060).

References

[1] D.M. Green, J.D. Burns, C.M. DeFusco, ICU management of aneurysmal subarachnoid hemorrhage, J. Intensive Care Med. 28 (2013) 341–354.
[2] R. Ayer, J. Zhang, Connecting the early brain injury of aneurysmal subarachnoid hemorrhage to clinical practice, Turk. Neurosurg. 20 (2010) 159–166.
[3] F.A. Sehba, J. Hou, R.M. Pluta, J.H. Zhang, The importance of early brain injury after subarachnoid hemorrhage, Prog. Neurobiol. 97 (2012) 14–37.
[4] P.J. Brouwers, D.W. Dippel, M. Vermeulen, K.W. Lindsay, D. Hasan, J. van Gijn, Amount of blood on computed tomography as an independent predictor after aneurysm rupture, Stroke 24 (1993) 809–814.
[5] P. Ascenzi, A. Bocedi, P. Visca, F. Altruda, E. Tolosano, T. Beringhelli, M. Fasano, Hemoglobin and heme scavenging, IUBMB Life 57 (2005) 749–759.
[6] G. Xi, R.F. Keep, J.T. Hoff, Mechanisms of brain injury after intracerebral haemorrhage, Lancet Neurol. 5 (2006) 53–63.
[7] E.E. Benarroch, Brain iron homeostasis and neurodegenerative disease, Neurology 72 (2009) 1436–1440.
[8] K. Poplawska-Domaszewicz, J. Florczak-Wyspianska, W. Kozubski, Update on neurodegeneration with brain iron accumulation, Neurol. Neurochir. Pol. 48 (2014) 206–213.
[9] C. Munoz-Bravo, M. Gutierrez-Bedmar, J. Gomez-Aracena, A. Garcia-Rodriguez, J.F. Navajas, Iron: protector or risk factor for cardiovascular disease? Still controversial, Nutrients 5 (2013) 2384–2404.
[10] J.Y. Lee, R.F. Keep, Y. He, O. Sagher, Y. Hua, G. Xi, Hemoglobin and iron handling in brain after subarachnoid hemorrhage and the effect of deferoxamine on early brain injury, J. Cereb. Blood Flow Metab. 30 (2010) 1793–1803.
[11] C.V. Nicchitta, J.R. Williamson, Spermine. A regulator of mitochondrial calcium cycling, J. Biol. Chem. 259 (1984) 12978–12983.
[12] Y. Kirichok, G. Krapivinsky, D.E. Clapham, The mitochondrial calcium uniporter is a highly selective ion channel, Nature 427 (2004) 360–364.
[13] H. Yan, D. Zhang, S. Hao, K. Li, C.H. Hang, Role of mitochondrial calcium uniporter in early brain injury after experimental subarachnoid hemorrhage, Mol. Neurobiol. (2014).
[14] J. Sripetchwandee, J. Sanit, N. Chattipakorn, S.C. Chattipakorn, Mitochondrial calcium uniporter blocker effectively prevents brain mitochondrial dysfunction caused by iron overload, Life Sci. 92 (2013) 298–304.
[15] J. Sripetchwandee, S.B. Kenknight, J. Sanit, S. Chattipakorn, N. Chattipakorn, Blockade of mitochondrial calcium uniporter prevents cardiac mitochondrial dysfunction caused by iron overload, Acta physiol. (2013).
[16] G.F. Prunell, T. Mathiesen, N.A. Svendgaard, A new experimental model in rats for study of the pathophysiology of subarachnoid hemorrhage, Neuroreport 13 (2002) 2553–2556.
[17] Q. Sun, Y. Dai, X. Zhang, Y.C. Hu, D. Zhang, W. Li, X.S. Zhang, J.H. Zhu, M.L. Zhou, C.H. Hang, Expression and cell distribution of myeloid differentiation primary response protein 88 in the cerebral cortex following experimental subarachnoid hemorrhage in rats: a pilot study, Brain Res. 1520 (2013) 134–144.
[18] Y. Dai, Q. Sun, X. Zhang, Y. Hu, M. Zhou, J. Shi, Cyclosporin A ameliorates early brain injury after subarachnoid hemorrhage through inhibition of a Nur77 dependent apoptosis pathway, Brain Res. 1556 (2014) 67–76.
[19] Z. Zhuang, M.L. Zhou, W.C. You, L. Zhu, C.Y. Ma, X.J. Sun, J.X. Shi, Hydrogen-rich saline alleviates early brain injury via reducing oxidative stress and brain edema following experimental subarachnoid hemorrhage in rabbits, BMC Neurosci. 13 (2012) 47.
[20] W.H. Tong, T.A. Rouault, Functions of mitochondrial ISCU and cytosolic ISCU in mammalian iron–sulfur cluster biogenesis and iron homeostasis, Cell Metab. 3 (2006) 199–210.
[21] H. Xia, Y. Cao, X. Dai, Z. Marelja, D. Zhou, R. Mo, S. Al-Mahdawi, M.A. Pook, S. Leimkuhler, T.A. Rouault, K. Li, Novel frataxin isoforms may contribute to the pathological mechanism of *Friedreich ataxia*, PLoS One 7 (2012) e47847.
[22] R.J. Ward, F.A. Zucca, J.H. Duyn, R.R. Crichton, L. Zecca, The role of iron in brain ageing and neurodegenerative disorders, Lancet Neurol. 13 (2014) 1045–1060.
[23] H. Ye, T.A. Rouault, Human iron–sulfur cluster assembly, cellular iron homeostasis, and disease, Biochemistry 49 (2010) 4945–4956.
[24] Y. Ke, Z.M. Qian, Brain iron metabolism: neurobiology and neurochemistry, Prog. Neurobiol. 83 (2007) 149–173.
[25] L. Zecca, M.B. Youdim, P. Riederer, J.R. Connor, R.R. Crichton, Iron, brain ageing and neurodegenerative disorders, Nat. Rev. Neurosci. 5 (2004) 863–873.
[26] M.W. Hentze, M.U. Muckenthaler, N.C. Andrews, Balancing acts: molecular control of mammalian iron metabolism, Cell 117 (2004) 285–297.
[27] T.A. Rouault, The role of iron regulatory proteins in mammalian iron homeostasis and disease, Nat. Chem. Biol. 2 (2006) 406–414.
[28] O.S. Chen, S. Hemenway, J. Kaplan, Inhibition of Fe–S cluster biosynthesis decreases mitochondrial iron export: evidence that Yfh1p affects Fe–S cluster synthesis, Proc. Natl. Acad. Sci. U.S.A. 99 (2002) 12321–12326.